nature biomedical engineering

Perspective

https://doi.org/10.1038/s41551-022-00998-9

Opportunities and challenges in the diagnostic utility of dermal interstitial fluid

Received: 28 April 2022

Accepted: 6 December 2022

Published online: 19 January 2023

Check for updates

Mark Friedel[1,7], Ian A. P. Thompson[2,7], Gerald Kasting[3], Ronen Polsky[4], David Cunningham[5], Hyongsok Tom Soh[2,6] ✉ & Jason Heikenfeld[1] ✉

The volume of interstitial fluid (ISF) in the human body is three times that of blood. Yet, collecting diagnostically useful ISF is more challenging than collecting blood because the extraction of dermal ISF disrupts the delicate balance of pressure between ISF, blood and lymph, and because the triggered local inflammation further skews the concentrations of many analytes in the extracted fluid. In this Perspective, we overview the most meaningful differences in the make-up of ISF and blood, and discuss why ISF cannot be viewed generally as a diagnostically useful proxy for blood. We also argue that continuous sensing of small-molecule analytes in dermal ISF via rapid assays compatible with nanolitre sample volumes or via miniaturized sensors inserted into the dermis can offer clinically advantageous utility, particularly for the monitoring of therapeutic drugs and of the status of the immune system.

Interstitial fluid (ISF) surrounds cells within tissue. It is the medium through which cells receive nutrients, secrete waste and communicate through molecular signals. By volume, the human body contains at least three times more ISF than blood[1]. Dermal ISF—that is, ISF within the skin—is commonly thought to be roughly equivalent to blood in terms of biomarker composition; hence, because it is present near the skin's surface, it could enable easier access to biomarkers without the pain or clotting associated with blood draws[2,3]. Virtually every analyte present in blood can be assumed to be present in ISF, including more than 92% of RNA species and over 90% of circulating proteins, with multiple studies stating that 99% of the proteins in blood are also present in ISF[4–6]. Beyond circulating proteins, ISF is also host to a small portion of proteins that are not present in blood[5].

Despite its apparent ease of access, ISF can be challenging to collect. Components of the extracellular matrix (ECM) within the interstitial space (in particular, collagen and glycosaminoglycans (GAGs)) can bind water, conferring ISF a hydrogel-like consistency[7]. Extracted ISF can provide valuable information, but the design of ISF-collection methods that produce accurate samples remains challenging. When fast sampling of large ISF volumes is attempted, in most cases the mesh-like ECM acts as a filter that hinders the extraction of large solutes[8] (but not of small molecules, such as glucose). This makes it exceedingly difficult to quantify the actual concentrations of large protein biomarkers such as cytokines, peptide hormones and immunoglobulins within extracted ISF samples. More generally, the physiological concentrations of analytes in ISF relative to their concentrations in blood remain poorly characterized.

The diagnostic utility of ISF has been increasingly explored. The most notable diagnostic application of ISF is in glucose monitoring for the management of diabetes. Microsensors within the dermis can continuously measure changing glucose levels in ISF with high accuracy and fast temporal resolution over several weeks. Also, continuous glucose metres relying on ISF are similarly accurate (even when not requiring blood-based calibration[9]) to finger-prick glucose metres using blood (typical mean absolute relative differences are less than 10%). This contrasts with more accessible biofluids (in particular, saliva, tears and sweat) which are associated with inconsistencies in sample collection arising from variable sample dilutions and compositions, and from other complications[10]. Because of the successes in the monitoring of glucose via ISF, increasing attention and research-and-development

[1]Novel Device Laboratory, Department of Biomedical Engineering, University of Cincinnati, Cincinnati, OH, USA. [2]Department of Electrical Engineering, Stanford University, Stanford, CA, USA. [3]The James L. Winkle College of Pharmacy, University of Cincinnati Academic Health Center, Cincinnati, OH, USA. [4]Nano and Micro Sensors, Sandia National Laboratories, Albuquerque, NM, USA. [5]Department of Chemistry and Physics, Southeast Missouri State University, Cape Girardeau, MO, USA. [6]Department of Radiology, Stanford University, Stanford, CA, USA. [7]These authors contributed equally: Mark Friedel, Ian A. P. Thompson. ✉e-mail: tsoh@stanford.edu; heikenjc@ucmail.uc.edu

efforts have been directed towards exploring the utility of ISF for diagnostic assays (either ex situ or in situ via wearable or implantable sensors).

In this Perspective, we overview the utility of ISF for diagnostic applications by exploring the opportunities and challenges of the use of dermal ISF as a biofluid that is potentially rich in diagnostic value. We provide cautionary insights, rooted in the incomplete understanding of how analytes partition into ISF. We refer to previous review articles for a detailed discussion on the flow of analytes into ISF[11], on microneedle devices for ISF sensing[12–14] and on specific applications such as therapeutic-drug monitoring[15]. We argue that when designed with a deep understanding of the properties of ISF, diagnostic applications based on biomarkers in it may prove advantageous for a wide range of biomarkers and diseases beyond glucose and diabetes.

Structure and composition of the dermis

As the outermost barrier of the skin (Fig. 1a), the epidermis is avascular and has the lowest ISF content (15–35% by mass) of the three main skin layers—epidermis, dermis and hypodermis[16,17]. The epidermis is approximately 100 μm thick at common ISF-access sites such as the arm or the abdomen, and is composed of four to five layers of different thicknesses and compositions, including the stratum corneum—a cornified outer layer that acts as a barrier to the transport of many compounds and prevents excessive water loss. The dermis consists of two sublayers (the papillary dermis, about 15 μm thick and highly vascularized[18], which supplies nutrients to the epidermis; and the 1–4-mm-thick gel-like reticular dermis) and has low cellular content, consisting mainly of fibroblasts and immune cells. Yet, its highest ISF content and proximity to capillaries makes it the best layer for accessing ISF. The hypodermis (also known as the adipose layer or the subcutaneous fat layer) is mainly composed of adipocytes, fibroblasts, connective tissue, nerves and arteries. As with the epidermis, its low water content, variable cellular composition and depth makes this layer less suitable for extracting ISF.

By mass, the dermis is approximately 70% water, of which 40% is ISF and 30% is bound water[17]. Bound water is confined through non-covalent bonding to the dense network of collagen, GAGs and proteoglycans that make up the dermis ECM (Fig. 1b), and therefore cannot be readily extracted. Because it acts as a size- and charge-dependent barrier to advective flow[19], and because bound water tightly limits convective flow[20], the ECM creates high hydraulic resistance within the dermis. High hydraulic resistance confers the skin many of its mechanical properties, but it imposes limitations for the sensing and extraction of ISF. Small molecules such as ions or glucose can diffuse into the microenvironment of bound water, but proteins and other macromolecules are hindered from accessing the dermis' bound-water fraction.

The dermis interfaces with systemic blood circulation through two web-like capillary plexuses that are fed by arterioles. The papillary capillary layer lies beneath the epidermis in the superficial dermis, whereas a deeper plexus lies between the dermis and hypodermis[16]. These capillary interfaces are inherently leaky[10], and serve as the source of nutrients and signalling molecules within ISF. Conversely, the lymphatics serve as a drain of fluid and analytes out of the dermis, ensuring that the tissue does not retain too much water (which would give rise to oedema). Dermal lymphatics are organized similarly to the capillaries but at a lower density[21]. They form a web-like network that passively collects fluid from the dermis. Lymphatic capillaries flow into lymphatic vessels, which connect to the lymph nodes where most of the collected fluid is processed by macrophages and returned to the bloodstream. Fluid flow through the dermis is driven by a descending hydrostatic gradient from positive capillary pressure (10.5–22.5 mmHg relative to atmospheric pressure)[22] to the negatively pressurized dermis (−1 to −4 mmHg)[23], and then removed by lymphatic suction[24]. Under homoeostatic conditions, fluid flow is unidirectional, from capillary to ISF to lymph[25]. The amount of serum volume being leaked into the interstitial space through the whole body varies between individuals and is in the range of about 1.8–8 l d^{-1} (refs. [16,25]).

The fraction of ISF content in the dermis that is accessible is small. For an estimated free-ISF content of 40% by volume, only 120 μl cm^{-2} of ISF is available in the thickest regions of the dermis (about 3 mm)[17]. The natural rate at which fresh ISF is introduced into the dermis is, however, a greater constraint on ISF extraction. Fluid flow through the dermis is hindered by high fluidic resistance and can most accurately be estimated on the basis of lymphatic clearance rate rather than capillary flow rate. For a measured lymphatic clearance rate of 8×10^{-6} ml s-cm^{-3} (ref. [26]) within a 3-mm-thick region of dermis over 1 cm^2 of skin area, the clearance rate would be only 0.96 nl s-cm^{-2} or about 60 nl min^{-1} cm^{-2}. To fully refresh the dermal ISF content (on the basis of a volume of 120 μl cm^{-2}), full fluid turnover without mixing (which does not reflect real-world conditions) would require more than 30 h. The transport of solutes into the dermis is therefore not solely driven by the advective flow of water and must be aided by diffusion.

Partitioning of analytes in dermal ISF

Because blood is the progenitor of interstitial fluid, to understand how analytes enter the interstitial space requires understanding of the barrier function of the capillary wall (Fig. 1c). The capillaries surrounding the dermis are majorly non-fenestrated continuous capillaries rather than the leakier fenestrated capillaries found in the fingers and other extremities and in some internal organs. The luminal side of continuous capillaries comprises a single layer of endothelial cells. The inter-endothelial junctions (IEJs) between cells are connected mainly by cadherin junctions and by some tight junctions that modulate the permeability of the capillaries to solutes[27]. The interior of the capillary endothelium is coated with glycocalyx (the major charge barrier of the capillary wall, consisting of GAGs, proteoglycans and negatively charged adsorbed proteins[28]). Also scattered along the endothelial membrane are caveolae (the small invaginations of the lipid bilayer that act as a shuttle system for transcytosis[29]). Size selectivity of the lymphatic barrier has minimal impact on the composition of analytes in ISF; in healthy tissue, the lymph regulates fluid pressure, yet it is much less restrictive to analytes. Therefore, the capillary structure largely determines the concentration of most solutes in the dermis[30–32].

Paracellular transport and transcellular transport are two dominant pathways for the partitioning of analytes from blood into ISF (Fig. 1c). In paracellular transport, analytes pass through junctions between cells in the capillary endothelium, hence the pathway is both diffusive and advective. Also, the properties of cadherin and of tight junctions lead to strong selectivity for analyte size. In transcellular transport (that is, transport directly through endothelial cells), hydrophobic molecules diffuse directly through the plasma membrane, whereas hydrophilic species rely on vesicular transport across the cell after being endocytosed at caveolae. Vesicular transport can occur with the molecule in bulk fluid phase or be mediated by specific receptor binding[27].

Because capillaries are inherently leaky through a number of extravasation pathways, almost all analytes that are present in blood are also present in ISF. Hence, when evaluating ISF as a diagnostic biofluid, the challenge is to determine the relative concentration of an analyte in ISF with respect to that in blood (Fig. 1d) rather than whether the analyte is present in ISF. Size, charge, percentage of analyte bound to serum proteins and other biomolecular properties will dictate the analyte's relative abundance in ISF. For small hydrophilic molecules having molecular weights greater than about 100 Da, the dominant transport mechanism from blood to ISF is paracellular diffusion. Small hydrophilic molecules such as water and short-chain alkanols are also quite membrane-permeable and can diffuse transcellularly[26]. For small hydrophobic molecules, the dominant route is transcellular diffusion, unless they are protein-bound. The IEJs of dermal capillaries predominantly consist of cadherin junctions, which permit

https://doi.org/10.1038/s41551-022-00998-9

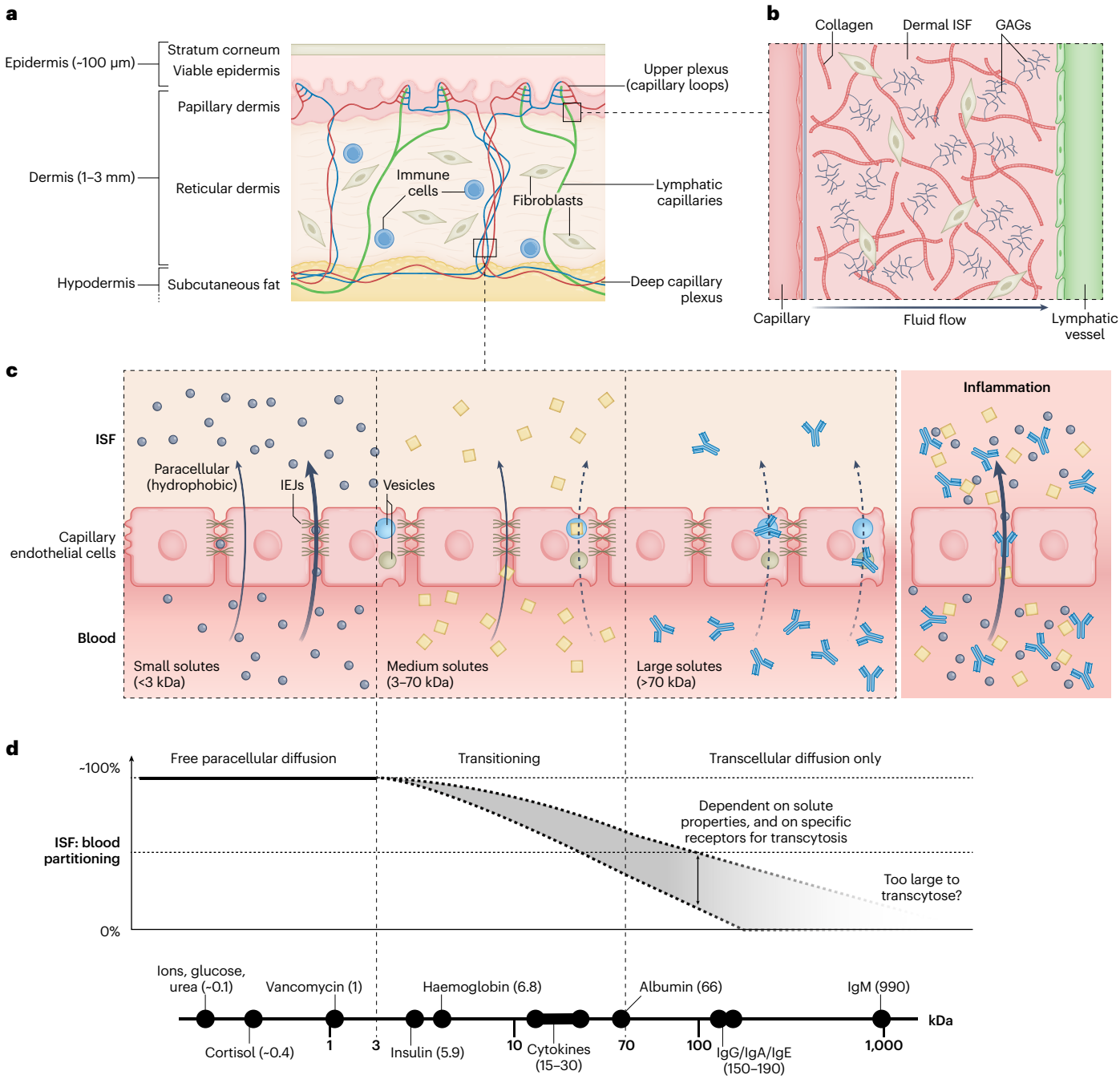

Fig. 1 | Structure of the skin, and analyte partitioning into dermal ISF. a, The overall structure of the skin. **b**, Microstructure of the mesh-like dermis, where pressure gradients drive flow between capillary blood and lymph. Fluid resistance comes from the dense extracellular matrix, which is composed of collagen and GAGs. **c**, The capillary interface consists of a single layer of endothelial cells, which controls the transport of analytes between the blood circulation and ISF. Depending on molecular size, transport across this interface can occur either via paracellular diffusion through IEJs between cells, or via transcellular transport through cellular vesicles. Inflammation disrupts the capillary endothelium, leading to enhanced extravasation for analytes of all sizes and distorting ISF partitioning (relative to homoeostatic conditions). **d**, The relationship between extravasation pathways and molecular size leads to differences in the partitioning of molecular species between ISF and blood. The graph depicts the general trend of molecular-size-dependent partitioning and lists the molecular sizes of a few clinical biomarkers. Panel **d** adapted from ref. [27] under a Creative Commons license CC BY 4.0.

the diffusion of small solutes (<3 kDa) regardless of their charge[27,33]. The remaining IEJs are tight junctions that block all but the smallest of analytes (<4 Å) in their closed state; still, these exhibit frequent breaks and undergo remodelling that permits the leakage of larger molecules[27,34,35] (however, this has not been rigorously proven for the capillary endothelium). Owing to constant tight-junction remodelling, cadherin junctions form the dominant size-selective filter of advective and passive transport. For analytes in the range of 3–70 kDa, cadherins and tight junctions partially limit the passage of solutes. In this transitional size range, both transcellular and paracellular transport are important (Fig. 1c,d). Paracellular transport is hindered by cadherins and the luminal glycocalyx in a size-dependent manner, such that the partitioning of a biomolecule into the ISF roughly correlates with the biomolecule's diffusion coefficient and size[8]. For example, 30% of

the movement of moderately large, negatively charged molecules such as albumin (66 kDa) occurs via paracellular routes, with the remaining 70% occurring via transport vesicles[36]. Accordingly, with respect to the concentration of albumin in blood, there is a 58% reduction of albumin concentration in ISF from rabbits[37] and a 52% reduction in ISF from tissue in the human leg[38]. Molecules larger than about 70 kDa have greatly reduced concentrations in ISF because their size prevents their diffusion through IEJs (the molecules are therefore transported transcellularly). Figure 1d summarizes the expected ISF content of different analytes relative to that in blood.

Charge state and hydrophobicity are also important determinants of the degree of transcellular and paracellular partitioning of biomolecules between blood and ISF. The negative charge of the luminal glycocalyx acts as a selective barrier against the diffusion of negatively charged molecules of intermediate size (3–70 kDa)[39,40]. By contrast, neutral and positively charged drugs and proteins should exhibit somewhat higher ISF partitioning. However, disruption of the charge barrier, in particular during inflammation (Fig. 1c), may affect partitioning. In general, hydrophobic small molecules can quickly penetrate the lipid bilayer of endothelial cells and transcellularly diffuse into ISF. However, the lipid bilayer or fatty tissue in the skin may also act as a sink for analytes with high hydrophobicity, slowing their rate of change in the dermis with respect to that in blood. This complex trade-off between enhanced lipid-bilayer penetration and decreased escape kinetics has been investigated for hydrophobic solutes in vitro[41], and the kinetics of hydrophobic molecules characterized in vivo in the context of designing drugs for rapid uptake by gut tissue or for permeation through it[42,43]. Also, many clinically relevant small hydrophobic analytes (such as steroid hormones or drugs) bind strongly to albumin and to other large carrier proteins with lower ISF penetration. For example, cortisol is about 95% bound to transcortin[44], and more than 50% of orally delivered drugs are more than 90% protein-bound[45]. Hence, correlations between the content of these species in ISF and in blood heavily favour their unbound concentration, unlike typical blood measurements of total concentration. The binding state of an analyte also determines its bioavailability in ISF and how available it is to a sensor. In fact, for most analytes, the unbound concentration is also the concentration of its biologically active 'portion' and is therefore a more clinically meaningful metric than its total concentration.

Effects of skin disruptions on the composition of ISF

The disruption of the epidermis, including attempts to sample or probe ISF, elicits an immune response that drives ISF away from homoeostasis. Here we limit the discussion to disturbances of the superficial subcutaneous tissue (less than 10 mm deep), as readings from deeper penetrations are not as diagnostically relevant, cause greater bleeding and produce a more substantial local response. Inflammation of the skin is induced by disruption of the transepithelial electrical potential[46], which triggers the release of inflammatory factors (such as bradykinin and histamine). These factors disrupt the glycocalyx charge barrier and induce cellular contraction, leading to the formation of leaky capillary gaps that eliminate the size-exclusion function of the capillary–ISF interface for solutes of up to 2,000 kDa (ref. [47]). This can result in the unimpeded diffusion of most proteins and virtually all immunoglobulins, with increased transport through both transcellular and paracellular pathways (Fig. 1c). Hence, the inflammatory response may distort analyte concentrations in the ISF and undermine the accuracy of any sampling approach that disrupts the dermis.

Current understanding of penetration effects on analytes in ISF is limited, with a heavy focus on skin inflammatory responses and their effects on analytes such as cytokines. Some reports of microneedle penetration into the skin have described short-lived skin erythema for 1 h (ref. [48]). Further work showed that non-immunogenic damage to the epidermis led to the release of pro-inflammatory cytokines in the epidermis within 1 h. However, cytokine levels in the dermis were not affected until 6 h after perturbation, with no change in mRNA-expression levels[49]. Other studies have found that microdialysis probes placed about 700 μm deep into the skin elicited increased concentrations of IL-6 and IL-8 at the site of implantation 3 h and 6 h post-insertion, respectively[50]. Together, these data suggest that the inflammatory response induced by any ISF-accessing device could substantially affect the measured analyte concentrations. However, this effect is likely to be transient and highly dependent on how the device interfaces with the dermis. Indeed, the extent of the reaction of the skin to even the gentlest epidermal penetration is highly dependent on a range of factors, including what penetrates the skin, for how long, the number of penetrations, an individual's skin response and the use of anti-inflammatories. We have therefore only provided a brief survey of the range of effects on ISF-biomarker levels that have been observed. It is also relevant to stress that for any given device, these outcomes represent what may happen and not necessarily what will happen.

Challenges in obtaining true ISF via extraction

Extracted ISF is valuable because of its low invasiveness, its exclusion of interferents such as blood cells and its improbability of clotting. However, extracting ISF in meaningful volumes is difficult for two main reasons: volume and filtration.

There are only 120 μl of ISF available per cm^2 of skin in the thickest regions of the dermis. Although approximately 100 μl quantities are sufficient for most laboratory techniques, in practice most extraction techniques collect volumes on the order of 1–10 μl. Such miniscule volumes are compatible with some high-sensitivity analytical methods (such as mass spectroscopy and some enzyme-linked immunosorbent assays)[51], but are inadequate for many rapid point-of-care diagnostic tests. This is a substantial limitation when ISF extraction is compared to capillary-blood sampling methods that can rapidly provide 100 μl samples[52]. Furthermore, ISF volumes can only be replenished from blood at a limited rate.

The application of force during sample collection can lead to a filtration effect that lowers analyte concentrations in the collected samples. This is because water and small analytes are pulled across these size-selective interfaces more rapidly than large biomolecules[53,54]. Lower extraction rates can circumvent this problem, but the required rates may be too slow to practically allow for point-of care uses or for continuous sampling from a single site. Yet multisite collection may be viable when collecting from the same tissue or with small and unfiltered analytes. For example, variability in multisite glucose measurements of ISF collected from the forearm has been shown to be negligible[55]. Still, numerous devices have been engineered for ISF extraction in vitro without accounting for the impact of constraints on in vivo extraction. For example, a calculation of vacuum extraction with 200 hollow microneedles in vitro can collect fluid at a rate of about 11 ml min^{-1}; however, in actual dermis, the poor hydraulic permeability of the ECM limits the extraction rate to a mere 6.7 μl min^{-1} at best when applying high-pressure suction via osmotic draw (supporting calculations are available as Supplementary Information). In what follows, we survey previously described ISF-extraction methods (Fig. 2 and Table 1) and the extent to which their success is undermined by volume and filtration constraints. For each of these methods, it is most important to consider whether the extracted sample contains useful information about the analytes of interest. We also consider whether the methods provide molecular information in a more compelling manner than a simple finger prick or a microneedle-assisted blood draw.

The wick method

One of the earliest ISF-collection methods involves inserting a wicking material such as nylon into the dermal space, allowing it to saturate with ISF and then removing it for analysis. Pre-saturated wicks are commonly used to collect protein or analyte content, but dry wicks can also be

https://doi.org/10.1038/s41551-022-00998-9

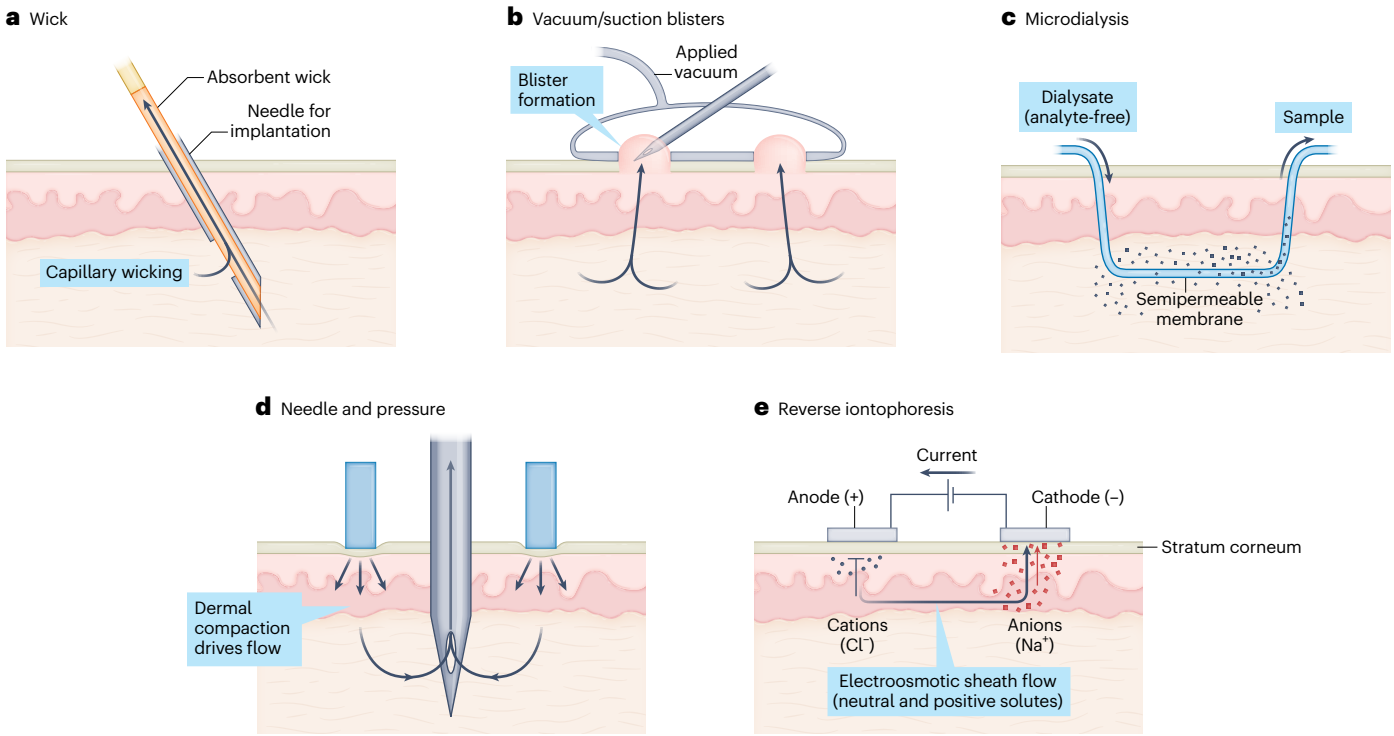

Fig. 2 | Methods for the extraction of ISF. a, Wick extraction inserts an absorbent wicking material into the dermis and relies on capillary action to saturate the wick with whole ISF or analytes for subsequent analysis. **b**, Suction blisters are induced by applying negative pressure to the dermis. The fluid within these blisters is then collected for analysis. **c**, Microdialysis relies on the diffusion of small solutes across a semipermeable membrane tubing implanted into the dermis. Samples are collected by slowly passing fluid through the implanted tubing and collecting the flow-through. **d**, Needle-based techniques insert a small needle into the dermis and apply pressure close to the insertion site to drive flow into the needle. This method enables the rapid collection of small volumes of ISF. **e**, Electroosmotic techniques such as reverse iontophoresis apply a voltage across the skin to drive the flow of charged solutes, causing the formation of sheath advective flow to the skin surface for subsequent sample collection or wearable-sensor measurements. Electroosmotic methods favour neutral and zwitterionic solutes.

inserted to collect whole ISF. In either case, there is not enough information available to determine the rate of ISF collection. Some studies have noted a protein-dilution effect in nylon wicks[56], whereas others have found that after 60 min, nylon wicks could adequately equilibrate with ISF in rats and humans[57,58]. However, this method is slow, invasive (it needs a needle for insertion) and requires further processing to collect the samples from the wick. Recent approaches for minimally invasive ISF extraction have coupled microneedles with wicking materials. For instance, a microneedle patch with an absorbent backing enabled the collection of 4 µl of rodent-tail ISF within 1 min after about 10 microneedle-patch insertions[51]. Another approach employed 100 hydrogel microneedles to passively wick ISF from the human arm. This method required only one insertion but could only collect 300 nl of ISF over 12 h (ref. [59]). Better polymer formulations could aid this collection method, and a similar device using a different polymer was able to collect 6 µl of ISF from mice in 10 min (ref. [60]). Overall, wicking methods are ultimately limited in the ISF volumes that they can collect.

Suction blisters

This method entails applying suction to continuously extract fluid. The force applied to the skin leads to cleavage of the dermal-epidermal junction[61]. Although the method is damaging to the tissue, high fluid-extraction rates can be achieved, allowing for collection rates of up to 5 µl min^{-1} cm^{-2} at −200 mmHg of applied vacuum. Unfortunately, the concentrations of large molecules in the samples that are collected this way differ considerably from their concentrations in serum[8,53,54] (the extent of this disparity is, however, reduced 24 h after the initial damage from vacuum suction[54]). The inconsistency of ISF composition obtained via vacuum and suction thus makes the methods unsuitable for the collection or continuous monitoring of large-molecule analytes. Related methods reduce invasiveness by first creating micropores in the skin using laser ablation or microneedles, followed by the application of lower pressures to extract small quantities (a few microlitres) of ISF per hour[3,62] (Table 1, row 'Micropores and suction').

Microdialysis and ultrafiltration

In this method, a semipermeable membrane is inserted into the dermis, allowing for the collection of whole ISF or of its analytes. Microdialysis uses flowing fluid to collect analytes from the dermis, whereas ultrafiltration applies vacuum to collect fluid. Ultrafiltration probes can be implanted for long-term use and have achieved collection rates of up to 50 µl h^{-1}. However, they rely on the highly invasive implantation of a large trocar into the skin. In both methods, biofouling of the membrane is a concern[63] (especially for microdialysis, which generally employs molecular-weight cut-offs of <3 kDa). Furthermore, at typical extraction rates, analyte concentration in fluid collected in microdialysis is typically 5–10-fold less than the actual ISF content[63]. Despite the challenges, these techniques are often employed to generate data for the US Food and Drug Administration (FDA) and other regulatory bodies when assessing small-molecule drug pharmacokinetics[64]. Also, a recently developed wearable microdialysis-based glucose sensor[65] might be used to continuously run assay-like tests. Still, in most cases, the complex design and components required for these devices make them less viable for biosensing than other minimally invasive indwelling sensors.

Needle-based extraction

A far simpler ISF-collection method involves inserting a small-gauge needle into the dermis and the application of pressure adjacent to the needle. A ring-shaped fixture is usually employed to minimize dermal

https://doi.org/10.1038/s41551-022-00998-9

Table 1 | Key properties of methods for the extraction of ISF

	Mechanism	Volume, rate and frequency	Dilution effects	Challenges	Outlook
Wick method[56–60]	Capillary wicking into a porous material.	1–10 µl in 1–10 min. Single extraction.	Dry wicks can achieve dilution-free sampling of ISF.	Conventional techniques are invasive and require bulky implantation of wicks. Requires post-processing.	Minimally invasive microneedle wicks and hydrogels for the collection of low-volume undiluted ISF samples could be valuable as point-of-care or at-home diagnostics.
Suction blisters[8,53,54,61]	Pressure-induced blistering, followed by needle-based sampling of the blister fluid.	5 µl min^{-1} cm^{-2}, continuously. Hundreds of microlitres within about 1 h. Single extraction.	High pressure can cause local damage and inflammatory responses, distorting analyte concentrations. Small molecules (less than 3 kDa) are unaffected.	A high degree of tissue damage leads to large differences in protein and metabolite content.	Limited use owing to a high degree of tissue damage and to distorted biofluid contents.
Microdialysis and ultrafiltration[2,63,65]	Small molecules diffuse across a semipermeable membrane and are collected by flow or vacuum.	Microdialysis: 0.1–10 µl min^{-1}, continuously. Ultrafiltration: tens of microlitres per hour, continuously.	Limited to small-molecule analytes (usually less than 3 kDa). A flow-rate-dependent 5–10-fold dilution is typical.	Extraction is relatively complex and invasive, which constrains its use for point-of-care or rapid diagnostics. Difficult with large or lowly abundant biomolecules.	Continued use for data collection in clinical trials involving small molecules until a less-invasive alternative arises.
Needle-based extraction[4,55,66]	Insertion of a small-gauge needle and application of pressure to drive the collection of fluid into the needle.	0.5–3 µl per needle within 1–10 min. Scales with the number of needles used. Single extraction.	A low volume and a low collection rate, yet dilution-free sampling.	Viable as a research tool, yet limited potential for clinical applications (when more convenient ISF-extraction methods are unsuitable).	Used in omics studies in humans. Valuable for studying undiluted ISF.
Reverse iontophoresis (electroosmosis)[10,69,70]	An electrical potential applied across the skin draws small ISF analytes along with advective flow.	Continuous extraction. Achievable rates are unknown but low.	For glucose, up to 1,000× dilutions have been observed. Likely to be unviable for large molecules owing to severe dilution.	Severe dilutions of analytes.	Of limited use owing to severe dilutions and to commercial challenges.
Micropores and suction[3,62]	Microneedles or laser ablation are used to create small holes in the skin, and suction is applied to collect ISF.	Continuous extraction at 5–15 µl h^{-1} after 1 h of applied suction. A single extraction yields about 2 µl in 20 min.	Minimal glucose dilution. Protein concentrations have not been reported, but inflammatory effects may be less prominent than with the use of suction blisters.	Requires further understanding of the effect of pressure on dilution effects and on inflammatory responses. Multiple components (for pore creation, suction and measurement) that are challenging to integrate.	Used in omics studies in humans and for the characterization of ISF. Cumbersome for point-of-care use owing to the many components needed. For large molecules, dilution and pressure effects may affect its viability.
Capture needles[67,68]	Needles or microneedles coated with antibodies are inserted in the dermis to capture specific biomarkers.	Single extraction, with no appreciable volume extracted.	No dilution. Quantification of analyte binding at a single timepoint. May not be suitable for the quantification of highly concentrated molecules if the device is fully saturated.	Only collects a single target molecule if only one antibody is used. Difficult to apply to most uses in the analysis of ISF.	Potential uses in the quantification of proteins in ISF for diagnostic applications. A simplified analysis for ex vivo uses would enable rapid point-of-care applications.

compaction in the vicinity of the microneedle, thus leading to lower fluidic resistance and improved extraction. The method provides volumes up to about 1 µl of fluid, which can be collected in seconds[66]. Modifications of this method for long-term, capillary-driven collection include the addition of capillary tubes as a reservoir, as well as the use of multiple needles to collect higher volumes of ISF, which can result in extraction rates of 2.6–5.3 nl min^{-1} per needle[4] (these rates were used to collect qualitative data of protein content, yet it is uncertain whether the method affected analyte partitioning). Another finding from this method is that cycles of repeated pressure and relaxation reduce the ISF time-lag when measuring rapidly changing blood glucose levels[55]. An emerging variation of the needle-based method uses receptor-coated microneedle patches to bind target analytes in situ, followed by patch removal and ex vivo analysis without the need to collect substantial fluid volume[67,68] (Table 1, row 'Capture needles').

Reverse iontophoresis

Reverse iontophoresis (also known as electroosmosis) uses voltage applied across the skin to generate electroosmotic flow of ISF through the epidermis to the surface of the skin via paracellular pathways, with

the negatively charged plasma membranes promoting the formation of a moving sheath of Na^+ ions. However, as expected from the paracellular route, electroosmotic methods collect samples in which analytes are more dilute than in physiological ISF. This is in part owing to the sieving effect of the ECM and IEJs, as well as to the method's implicit bias towards neutral or zwitterionic molecules, whose motility is largely based on fluid flow[10,69]. For example, the glucose extracted via reverse iontophoresis by the GlucoWatch Biographer, which uses two gel pads placed on the skin and cycled with direct-current potential, is typically about 1,000-fold more dilute than physiological levels[70]. As such, the resulting sample will differ considerably from true ISF, thus complicating sample analysis.

Coupling sensors to the dermis

Rather than the time-limited 'snapshot' that ISF-extraction methods provide, sensors coupled directly to the dermis could enable continuous monitoring with minimal effort. However, sensors put heavy demands on the particular molecular-measurement mechanism that they employ. For most practical continuous monitoring applications, sensors must track rapidly increasing and decreasing analyte levels directly in biofluids without the need for washing, reagent addition or mixing. Hence, sensors that can reliably measure analytes directly in ISF have been dedicated almost entirely to continuous glucose monitoring (CGM) and to a handful of research applications. In what follows, we describe current strategies, except for methods that employ spectroscopic techniques, to non-invasively and optically monitor ISF from outside the skin (it is unclear whether spectroscopic approaches can provide clinically relevant data).

CGM stands out as the only clinically adopted application of ISF-based sensors positioned securely within the dermis (also known as 'indwelling' sensors) that reach substantially deeper than microneedles. Its success can be attributed to the strong correlation between glucose levels in blood and ISF (because of diffusion, the concentration of glucose in these two fluid compartments equilibrates rapidly). Glucose is a hydrophilic small molecule (180 Da) that diffuses paracellularly from blood to ISF, with lag times of 5–10 min (ref. [71]). Also, tracking glucose concentration is straightforward because glucose can be oxidized with reactions that can be easily measured electrochemically. Many sensing mechanisms employ glucose oxidase, a naturally occurring enzyme that catalyses the oxidation of glucose (either alone or in conjunction with mediators that produce products that can be measured with indwelling electrodes[72]). Moreover, the relatively high glucose concentration in vivo (millimolar) helps to circumvent interference from other redox-active small molecules. Ref. [73] provides a comprehensive understanding of how these sensors work. In brief, the devices are adhered onto the upper arm or abdomen, and a small electrode coated with enzymes and a protective membrane (the sensor) is inserted into the subcutaneous space by an injector needle (Fig. 3a). Measurements are accessed via Bluetooth connection to a smartphone or to a dedicated scanner, and provide the individual with their current glucose level, rate of change and hours of glucose-concentration data (Fig. 3d). Factory-calibrated sensors (such as those from Abbott and Dexcom) are more accurate (mean absolute relative differences of 9.4% and 9.8%, respectively[73]) than many traditional finger-stick measurements. However, the longevity of these sensors is limited by the foreign-body response, which leads to fibrotic encapsulation of the implanted sensor. Over time, encapsulation limits the diffusion of glucose to the sensor surface, increasing delay times and diminishing sensor responsivity[74]. Moreover, the 14 d turnover of the stratum corneum can affect device adhesion[75], and sensor drift also limits their lifetime. Hence, these sensors for CGM require replacement and reinsertion of a new device at a new location a few times per month (7 d for Medtronic sensor, 10 d for the Dexcom sensor and 14 d for Abbott's) to maintain accuracy.

Implanted sensors are typically placed subcutaneously into the upper hypodermal space via injection with a needle-like device (Fig. 3b). These devices offer longer lifetimes alongside other advantages in terms of minimizing patient inconvenience of repeated sensor insertion. There is currently one approved implantable device for CGM designed for long-term biosensing. Rather than using an enzymatic mechanism, this CGM (marketed by Senseonics) uses a fluorescence-based polymer to detect glucose. The device is FDA-approved for 90 d of wear (but lasts for up to 180 d) and maintains similar accuracy to wearable CGMs over a longer time. However, it requires calibration with the aid of finger-prick blood testing twice daily[76–78]. Because of their longer lifetime, these sensors may have lower associated costs than traditional CGMs: US$250 for the implantation and removal procedures, in addition to the cost of the implant itself (variable), compared with an estimated cost from 2018 of US$1,368 for 90 d of use of a traditional CGM[79,80]. One drawback of the current generation of implanted devices is that they require the use of an external reader above the skin, which makes them only marginally simpler than conventional wearable devices for CGM; Bluetooth-enabled implantable sensors would eliminate the need for a wearable reader. Also, future devices may employ multiple enzymatic sensors for glucose[81]. Another implantable sensor (developed by Profusa and available in the European Union) provides subdermal local-tissue measurements of tissue oxygen levels in patients with ischaemia, with a hydrogel polymer-based fluorescent sensor that functions accurately for up to 95 d (ref. [82]). Currently, the need for quarterly device implantation and extraction means that implantable devices hold only marginally greater value relative to wearable sensors for long-term and short-term use. However, as sensor technology improves to produce longer-lasting sensors, it is likely that these devices will become a key component of ISF-based biomonitoring. Still, it is difficult to envision how sensors relying on optical measurements using analyte-responsive polymers may adapt to analytes that are much larger than the small molecules (<200 Da) measured with current technology. This would require exposing the sensor to increased risk of fouling and degradation.

There is considerable research and commercial interest in the use of microneedles, that is, minimally invasive micrometre-scale needles that when piercing the skin, can only penetrate the dermis. Microneedles are typically designed with a length of less than 700 μm, such that insertion typically causes no local bleeding and minimal pain if any[83]. However, erythema and local inflammation can still occur. Much of the enthusiasm behind microneedles is associated with the opportunity to gain greater consumer acceptance than with the use of bulkier indwelling sensors. Furthermore, the use of microneedle arrays in drug delivery suggests that special insertion devices are not required for small arrays of microneedles, and that simple pressure on application can be adequate[84]. Still, specialized mechanical inserters may be required for the reliable insertion of larger arrays[85]. There are two general approaches for microneedles: either the sensors are situated on the needles themselves[86], or hydrogel or hollow-lumen microneedles are used to diffusively relay ISF analytes to a sensor placed outside the body. A wide variety of materials and fabrication methods have been devised for making microneedles[13]. Perhaps the biggest challenge microneedles face today is reliable coupling to the dermis. Considering a 600-μm-long microneedle, after accounting for 100 μm of dermal access (owing to the epidermis), skin defects that are tens-to-hundreds of micrometres deep and a skin peak-to-valley roughness of about 100 μm (which worsens in older users), it becomes clear that for any given array, only some microneedles will be properly inserted in the dermis whereas others may only reach the epidermis. Even when needles are properly seated in the dermis, they need to maintain this position. There are only two examples of continuous ambulatory ISF measurements[87,88]. Hence, more data are needed to inform critical design-and-use questions for microneedles that require defendable data. Partial dermal insertion can be particularly problematic for enzymatic sensors, whose signal depends on flux of analyte to the enzyme in the sensor; they can lead to false high or low signals

https://doi.org/10.1038/s41551-022-00998-9

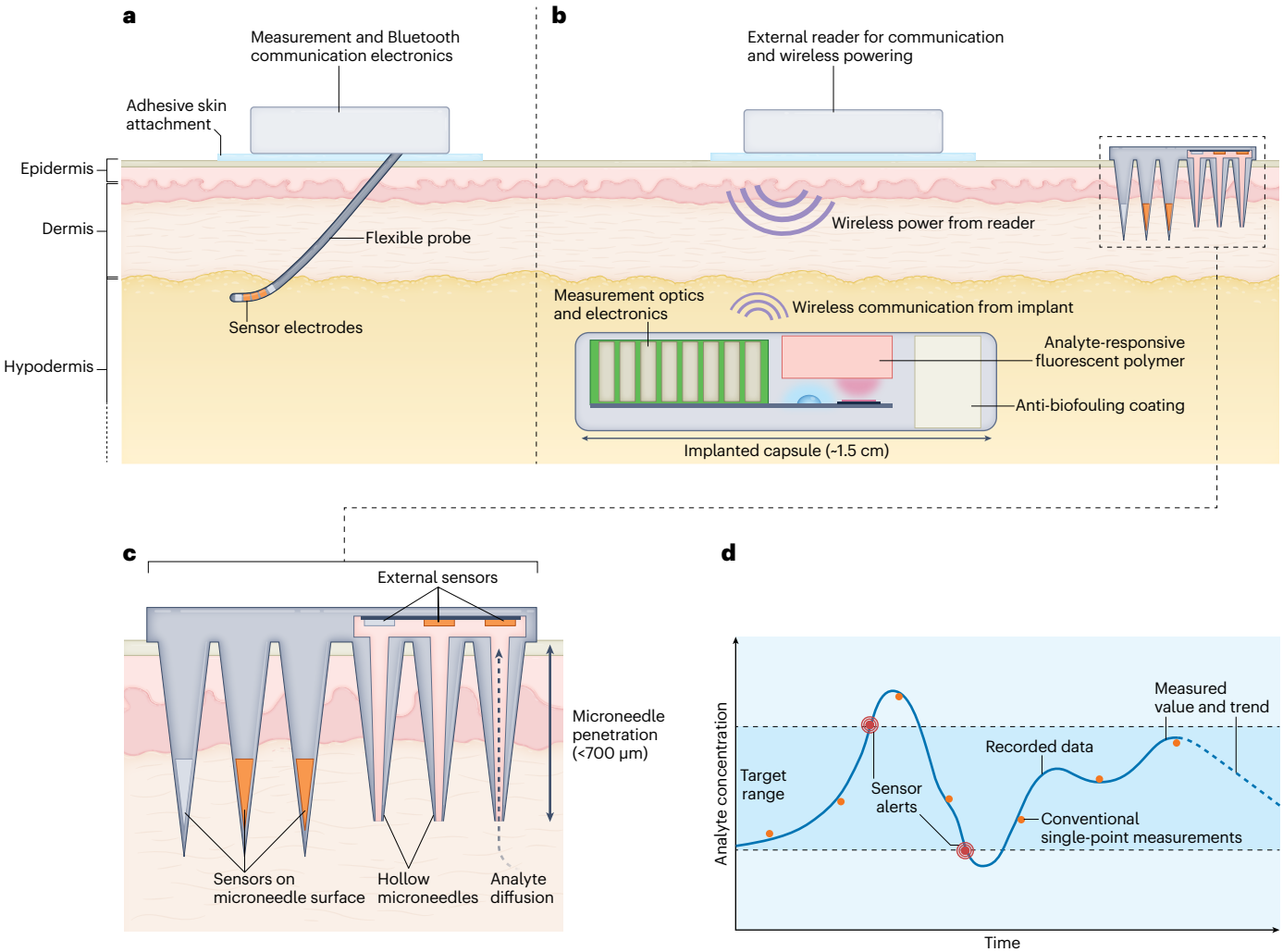

Fig. 3 | Sampling of dermal ISF for the continuous monitoring of glucose. **a**, Traditional devices for CGM rely on a single flexible probe that sits just below the dermis. Sensor electrodes near the tip of the probe measure surrounding glucose. A reader device adhered to the surface of the skin controls the measurements and stores the measured data, and then transfers the data to a smartphone or other receiving device. **b**, A sensor surgically implanted into the hypodermis uses an analyte-responsive fluorescent polymer to measure the concentration of the analyte. The implanted capsule device contains the electronics and optics necessary for the measurements, and requires wireless power from a reader device that sits above the skin. These devices rely on anti-biofouling coatings for greater longevity. **c**, An emerging class of microneedle-based sensors uses an array of small needles (<700 μm in diameter) to access the dermis with minimal pain. These can be designed with sensor electrodes directly on the needles' surface for sensing within the dermis, or as hollow or porous needles that allow for analyte diffusion from the dermis into external sensors on the other side of the microneedle patch. **d**, Representative CGM data from a sensor that interfaces directly with the dermis. The concentration of glucose is recorded continuously, can be read on-demand, and alerts can be relayed to the user when glucose levels approach the limits of the desired concentration range.

(that is, motion artefacts). For this reason, microneedles generally rely on redundant arrays of sensors. Also, large numbers of needles increase the perceived insertion pain[83] and may exacerbate the local inflammatory response.

There is a small but growing number of publications describing the design and use of integrated microneedle biosensors, some of them for clinically relevant applications. Most examples have used indwelling microneedle sensors that situate the sensing mechanism directly in dermal ISF. For instance, an indwelling enzymatic sensor for penicillin functioned for 6 h in healthy volunteers, with measurements similar to those collected by microdialysis[86]. A similar approach led to a wearable microneedle patch that enzymatically measured glucose, lactate and alcohol in the ISF of a few individuals, thus allowing for metabolic monitoring[88]. Additionally, electrochemical aptamers have been used in place of enzymes within a microneedle patch to perform therapeutic-drug measurements in rat ISF[89,90]. Moreover, another device employed hollow microneedles to couple ISF to an ex vivo enzymatic glucose sensor. It had a lag time of 17 min (which accounts for glucose's transport time from blood into ISF and for its diffusion time to the device) and gave comparable results to finger-stick blood measurements when used by diabetic patients[87]. Furthermore, recent research has used microneedles to overcome issues associated with ISF extraction by combining in situ analyte binding on a microneedle surface with the ex vivo analysis of bound analytes. This enabled the capture of post-immunization antibodies and of IL-6 at femtomolar concentrations in the ISF of mice[67]. A similar aptamer-based approach was used to monitor glucose levels in rats[68]. Still, owing to the limited data available, it remains unclear which design is better from a practical perspective if the goal is to sense a disease state: redundant (multiple) microneedle perforations and sensors in the upper dermis, or a single and fully adequate sensor insertion (as with current CGM devices).

Applications of ISF in diagnostics

There are numerous potential applications where ISF-based diagnostics would be advantageous, especially because ISF generally contains most blood-borne analytes of diagnostic interest. What is more, there are clinical scenarios where dermal ISF may be more suitable than blood draws. When considering the utility of ISF diagnostics, the following questions are particularly relevant. First, does the analyte of interest need to be measured continuously, rather than periodically in blood, urine or saliva? Second, is a tight correlation with blood-based measurements required, or the need is simply to scan an analyte to confirm a clinically relevant event? (For example, IL-6 for infection, troponin for cardiac damage or luteinizing hormone for ovulation.) Third, is the analyte present at a concentration that could be measurable with continuous sensors? (This would be in the nM-to-mM range with current technologies.) And fourth, is the measurement actionable such that it can convey clinical insights that enable or aid meaningful interventions?

The best first-order approach for predicting which analytes may correlate well between ISF and blood is a size-exclusion model of transport across the capillary interface. Because most small hydrophilic molecular species (such as ions, lactate, hydrophilic drugs and other common clinical markers) diffuse freely between the two compartments, their concentrations tend to match closely. An analysis of the temporal dynamics of the distribution of the drugs vancomycin (1,449 Da) and caffeine (194 Da) between ISF and blood revealed a strong correlation, with a time lag between blood and ISF concentrations of about 10 min for both molecules (glucose has a similar lag time[12,59,62]). However, the correlation is not strong for all small molecules. For example, for lactate, which was believed to be a strong contender for ISF detection, concentrations in blood and ISF do not correlate well[91]. Still, the rapid equilibration of many small hydrophilic molecules suggests that most would be strong candidates for continuous monitoring in dermal ISF. Unfortunately for most protein biomarkers, correlations between their concentrations in blood and dermal ISF have not been fully characterized. One reason is that such measurements are confounded by two major factors. First, proteins are right at the size threshold where size-selective filtration occurs in the capillary-wall structure (Fig. 1d). Second, sampling methods are often implemented in such a manner that pure dermal ISF is not being collected. However, the degree of protein filtration is sufficiently consistent for ISF measurements to be predictive of blood concentrations[67]. For instance, correlated enhancements of the cytokine IL-6 (about 25 kDa) were seen between microneedle-extracted ISF and serum samples in the presence and absence of endotoxin-induced shock. On endotoxin injection, the levels of IL-6 rose more slowly in ISF (approximately 2.5 h) than in serum (approximately 1 h), indicating slower partitioning of this moderately sized biomolecule across the capillary interface. Moreover, in a comparison of anti-poliovirus IgG (approximately 150 kDa) titres between dermal ISF and serum in immunized rats, IgG concentrations in ISF were about 30% lower than in serum; still, the concentrations in the two compartments were linearly correlated across timepoints and subjects[51] (the dynamics of this correlation between ISF and blood concentrations during transient and rapid changes remain unknown because IgG measurements were only collected once per week). The homogeneity of protein concentrations in the dermis is also poorly understood. Up to 68% of the aqueous phase of ISF may be inaccessible to proteins larger than 66 kDa (ref. [92]) owing to the mesh-like characteristics of the ECM. In a worst-case scenario, this could lead to measurement inaccuracies or the increase in impedance of diffusion towards the sensor would cause increased lag times (rather than sensor failure).

A handful of 'omics' studies have assessed the similarity between the blood and ISF compartments across a broad range of analytes by subjecting microneedle-extracted ISF to proteomic[5], metabolomic[62] and transcriptomic[4] analyses. These studies have revealed that the fraction of molecular species observed in blood, but not in ISF, is remarkably small: only less than 2% of the species cannot be detected in ISF across all classes of biomarkers. Conversely, only about 5% of the proteins and 10% of the metabolites and RNA transcripts were found to be unique to ISF. These species include numerous clinically relevant biomarkers, which suggests that ISF may offer unique information for understanding physiological processes occurring in the skin[62]. Exosomes (secreted extracellular vesicles of diagnostic interest) are over tenfold more abundant in ISF than in plasma. This suggests that such specimens could be ideal for exosomal profiling; still, whether exosomes in ISF hold value for the study of cancer, cardiovascular diseases and other diseases remains uncertain[4]. Samples of ISF could thus prove valuable for omics studies and for personalized medicine. Many biomarkers (besides those described here) may exhibit strong correlation between their ISF and blood concentrations. In the next two subsections, we highlight two applications for which we speculate continuous ISF sensing can succeed.

Continuous molecular biosensors

Despite the wide array of clinically relevant analytes present in ISF, diagnostic applications are limited by the lack of molecular mechanisms that can sensitively and specifically detect these analytes. In fact, the literature on sensors is dominated by in-vitro-only demonstrations that lack in vivo validation owing to substantial challenges in implementing technologies that are sample-preparation-free, that overcome the volume-and-flow-rate limits intrinsic to ISF and that maintain functionality in a complex biofluid. Furthermore, publications that have presented in vivo data often lack a direct comparison of the analyte levels in ISF and blood. We have identified only three sensor formats for continuous ISF sensing in vivo for which there are substantial data on analyte-concentration correlations between ISF and blood in humans or animal models, and across multiple analytes with clinically relevant sensitivity and robust specificity: ion-selective electrodes, electrochemical enzymatic sensors and electrochemical aptamer-based sensors whose key characteristics are outlined in Table 2. Because ion-selective electrodes are currently limited to the detection of small electrolytes[93], in what follows we focus on the two remaining types of electrochemical sensor.

Enzymatic sensors measure the product of a catabolic reaction (Fig. 4a). This is a mature technology, with multiple signal-transduction modalities available for numerous target analytes[94]. However, these sensors face challenges associated with longevity (with a few exceptions, such as sensors for glucose oxidase), limits of detection that are higher than the physiological analyte concentrations and cross-reactivity (this is the case for acetaminophen in sensors for CGM)[95]. Enzymes are also highly analyte-specific and typically not generalizable to multiple analytes. Additionally, because the scope of enzymatic ligands is generally limited to small molecules, enzymatic sensors are not suitable for the continuous detection of protein biomarkers.

Electrochemical aptamer sensors measure the binding and dissociation of a target analyte to a redox-tag-functionalized aptamer (Fig. 4b). Hence, they can be applied to sensing small molecules (hundreds of Da) and proteins (more than 10 kDa), and can achieve limits of detection matching in vivo concentrations (in the pM-to-μM range)[96]. Longevity is the biggest limitation for electrochemical aptamer-based sensors; few last more than 24 h in blood[97,98] but emerging work is suggesting that greater than 1 week longevity is possible[99]. Affinity-based sensors that employ protein receptors in place of aptamers may provide equivalent generalizability to aptamers as well as improved longevity, owing to a lack of nuclease susceptibility and to the inherent biocompatibility of naturally occurring proteins such as IgG. However, protein receptor sensors have not yet been tested in vivo to the same extent as enzymatic or aptamer sensors[100]. The steps required for the maturation of aptamers as continuous sensors for in vivo applications are outlined in ref. [96]. On the basis of current aptamer sensor technology, we envision

Table 2 | Key characteristics of technology for continuous biosensing

	Ion-sensitive electrodes	Enzymatic sensors	Aptamer-based sensors
Measurement mechanism	Potentiometric sensing of the changing Nernst potential of the electrochemical cell.	Amperometric detection of products of the enzymatic reaction.	Detection of changes in electrical current resulting from a conformational change in affinity receptors.
Suitable analytes	Electrolytes, such as Na^+, K^+, Cl^-, Ca^{2+}, Mg^{2+} and Li^+.	Small molecules, such as glucose, lactate, creatinine and urea, that act as enzyme substrates.	Small molecules, drugs and proteins.
Sensitivity	mM.	μM to mM.	nM to mM with DNA-based aptamers.
Molecular specificity	Highly selective between electrolytes, conferred by choice of ionophore.	Can be susceptible to interference from electroactive species (such as acetaminophen, uric acid and ascorbic acid in CGM).	Usually selective except for close molecular analogues. Selectivity can be determined by the stringency of aptamer selection.
Challenges	Limited to charged electrolytes and elements.	Relies on adapting natural enzymes. Needs substantial enzyme engineering for long-term stability.	In vivo demonstrations currently limited to hours at most, and sensor longevity improvements are still at the benchwork stage[99].
Stage of development	Implemented in many wearable sweat-based devices. Not generally used in an implanted format.	Currently FDA-approved and in use for CGM applications.	Demonstrated in vivo with rodents for the continuous detection of drugs in circulating blood, but only for <1 d.

a variety of potential applications—in particular, therapeutic-drug monitoring and the monitoring of the immune system—that may benefit from the continuous monitoring of ISF.

Therapeutic-drug monitoring

Electrochemical aptamer sensors can accurately quantify in vivo exogenously administered drugs, including vancomycin[101], kanamycin, ampicillin[102] and doxorubicin[103]. This suggests an outstanding opportunity for advancing personalized drug-dosing through therapeutic-drug monitoring. Many commonly used drugs have a narrow therapeutic window, outside of which dosing is either too low to elicit a therapeutic effect, or higher than can be tolerated without side effects. Interpatient variability in pharmacokinetics and in protein binding exacerbates the dosing challenge. Hence, the ability to regularly monitor administered drug concentrations and to adjust patient care correspondingly would aid the safe and effective use of therapies[104–107].

Therapeutic-drug monitoring in dermal ISF (rather than in blood) could improve both the ease and accuracy of the measurements. Drug concentrations in ISF may provide more representative measurements of drug tissue penetration when the target resides in the dermis (as is the case for anti-infectives and anti-inflammatories[108]). In this case, ISF-based measurements can increase the accuracy of therapeutic-drug monitoring by avoiding systemic and local effects that limit the accuracy of plasma-based measurements[15]. The extent of tissue penetration of systemically administered drugs can vary widely across patients; and, even if a therapeutic-drug-monitoring approach is successful at maintaining the desired drug concentration in blood, the actual drug exposure of the target tissue may be inadequate. This effect has been noted in studies of vancomycin, an antibiotic with a narrow therapeutic window that is used widely in the treatment of methicillin-resistant *Staphylococcus aureus*. It has been observed that diabetic patients are approximately twice as likely to develop post-operative infections, even when prophylactic antibiotics are used[109]. Indeed, measurements of the degree of soft-tissue penetration for vancomycin administered to post-surgical patients using ISF microdialysis found a threefold lower tissue penetration in patients with diabetes than in non-diabetic individuals (3.7 mg l^{-1} vs 11.9 mg l^{-1})[110]. By contrast, there were no substantial differences in the plasma levels of vancomycin between the two groups. Studies in non-surgical patients confirmed the poor agreement between serum and ISF measurements for patients with diabetes[111]. This effect may be attributable to impaired microcirculation, and thus to restrictions in the perfusion of vancomycin into ISF[112] in the patients with diabetes. Monitoring the drug directly in ISF could therefore enable more accurate drug monitoring and reduce the rates of post-operative infection.

The acute physiological effects of surgery, sepsis, kidney injury and general trauma can also have complex effects on the tissue penetration of drugs. These conditions bring about a wide range of global physiological changes, in particular, changes in hormone levels that control vasodilation and water retention, cardiac-output and blood-pressure changes, and modulated renal clearance. All of these alterations affect the leakage of water and analytes across the capillary interface, both in the dermis and in other organs[113–115]. These effects can result in rapid distortions in the relationship between drug concentrations in circulation and in ISF, making blood-based measurements a poor representation of conditions in the dermis and in other organ tissues. Hence, measurements in dermal ISF may be a better option when investigating drugs that act on targets in the dermis. Yet, because perfusion through capillaries in the dermis is uniquely dynamic owing to capillary recruitment for thermoregulation favouring non-exchanging capillaries[116,117], the measurements may not have a direct correlation to perfusion changes in other organs. Still, measurements in ISF are likely to be a better predictor of perfusion changes than blood-based measurements.

One additional advantage of ISF-based therapeutic-drug monitoring is that aptamer-based and enzyme-based indwelling biosensors measure only the concentration of drug that is not bound to proteins. This better reflects the bioavailable 'active' drug concentration[118,119]. By contrast, many blood-based therapeutic-drug monitoring methods (such as mass spectroscopy) measure only the total drug fraction or require additional sample-processing steps to differentiate protein-bound from protein-unbound species. For example, vancomycin, has a sizable protein-bound fraction (20–50% (refs. [45,120])). Thus, plasma-based estimates of free vancomycin concentrations may vary substantially solely on the basis of the assumptions made about protein binding. Because protein binding is widely observed across almost all drugs[45], direct measurement of the free-drug fraction in ISF with an indwelling sensor would yield a far more accurate measurement of the bioavailable levels of a drug.

Monitoring the immune system

Another new frontier for biosensing might be the development of sensitive and rapid methods for the detection of the activation of host immune responses. In particular, the ability to measure the early stages of the cytokine storm would transform the safe and effective treatment

https://doi.org/10.1038/s41551-022-00998-9

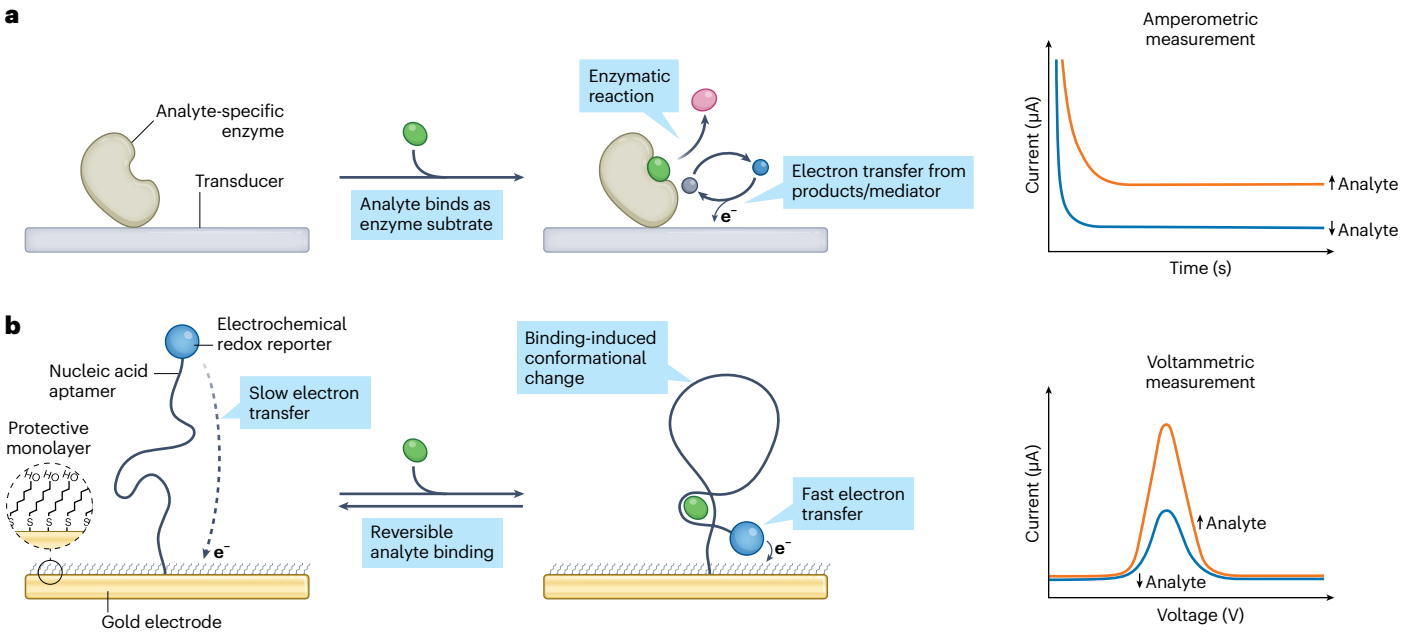

Fig. 4 | Two successful biosensor formats for continuous sensing. a, In an enzymatic sensor, the target molecule is broken down into products in a non-reversible reaction, wherein one of the products or a mediator carries an electrical charge that can be measured and correlated with the concentration of the target molecule. **b**, An electrochemical aptamer sensor binds and releases a target molecule as its concentration changes. When the target is bound, changes in the geometry of the sensor lead to changes in the rate of electron transfer, which can be correlated with the concentration of the target molecule.

of infections such as SARS-CoV-2 and influenza[121,122], and the management of chronic inflammatory disorders such as lupus and systemic juvenile idiopathic arthritis[123]. The skin has a rich immune-cell content and plays a critical role in the immune response; also, for some types of immune insult, concentrations of diagnostic cytokines in dermal ISF can be detected earlier than in blood. The viable epidermis is primarily composed of keratinocytes, which act as a systemic first line of defence by secreting cytokines (notably, IL-1) in response to external threats. This powerful early-warning system can instigate an inflammatory response before T-cell activation occurs, and can activate the immune system and produce systemic responses in distant organs[124]. Additionally, immunosurveillance-performing T cells are roughly three times more abundant in skin than in blood and contribute greatly to the pathogen response as well as to numerous autoimmune diseases[125]. This high density of immune cells has been shown to generate greatly enhanced local cytokine expression in animals and humans with inflammation. A comparison of the cytokine response in the dermal ISF and plasma of rats on induction of immune responses through either endotoxemia or ischaemia-reperfusion injury[126] (IRI) revealed that peak levels of IL-1β were about 300-fold higher in ISF than in serum in endotoxemia, and about 50-fold higher in IRI. Although increased IL-1β levels in serum could only be detected 20 min after IRI, measurements in ISF detected the cytokine within 3 min. TNF levels were also approximately 20-fold higher in ISF 3 min after IRI. Human studies have also substantiated the elevated cytokine content of ISF (for example, the concentrations of TNF and IL-1β, IL-6, IL-8 and IL-15 in samples of tissue and lymph fluid in the lower leg of healthy patients were higher in ISF than in serum[127]).

There is thus an important opportunity for next-generation biosensors to leverage ISF as a biofluid for the monitoring of the immune system and for the detection of increased local concentrations of secreted cytokines in the dermis. Point-of-care devices that can sensitively detect the initial stages of immune responses in the dermis would have a profound impact on the management of sepsis and other diseases for which early detection greatly decreases the risk of mortality[128]. This challenge is best suited for continuous sensors that operate over long timescales, as the initial insertion of the device may trigger transient disturbances in immune biomarkers that subside beyond about 6 h. Additionally, more research will be needed to improve the understanding of how local cytokine concentrations in the dermis correlate with systemic immune responses. In particular, it is not clear whether the increased cytokine levels occur only when the dermis plays a substantial role as the site of infection and inflammation, or whether the dermis acts as a sentinel of immune responses occurring elsewhere in the body. Moreover, for robust clinical performance, the low abundance of inflammatory biomarkers (typically, 1–100 pM)[129] in ISF will require dramatic improvements in the sensitivity of real-time biosensors.

Outlook

Advances in methods for accessing dermal ISF and for the continuous and rapid monitoring of biomarkers in it may facilitate implementations of personalized medicine. ISF holds promise as a blood proxy and as a biofluid that offers unique and rich insights into the perfusion of analytes, into disease states, and into local cell–cell signals that may not be discerned (or that cannot be discerned) by sampling blood. However, the path to the routine use of ISF in diagnostics is complicated. Table 3 outlines some of the fundamental questions that should be addressed when developing ISF-based sensors. In general, the high resistivity of the dermis to fluid flow limits both the maximum sampling rate and the total volume of physiologically representative ISF that can be easily extracted. ISF-extraction methods that exceed such a 'speed limit' may suffer from dilution and produce samples that are not representative of physiological ISF. Therefore, early successes have mainly involved small molecules (<3 kDa), which can rapidly partition from blood to ISF with minimal dilution. Proteins, RNA and other macromolecules (>30 kDa) are also potential sensing targets, but their concentrations in ISF are almost certainly lower than those in blood, and will thus require the development of extremely sensitive biosensing technology. Furthermore, continuous wearable sensors must function in undiluted biofluid; electrochemical biosensors can do so, but their short lifespan (<24 h) currently limits their viability as continuous biosensors. These difficulties should not deter research and development in ISF biosensing.

Table 3 | Guidance for the development of ISF-sensing technologies

Unmet need	Is there a substantial diagnostic need that is not served or that is served in a sub-optimal manner (such as accuracy, time, cost or convenience)? Will clinicians or patients act if provided with such diagnostic data?
Analyte	Do changes in the concentration of analyte in ISF correlate with changes in its concentration in blood or with other gold-standard measurements that serve the diagnostic need? Will the local response to ISF sampling affect analyte measurements negatively? For continuous monitoring, does the analyte partition into ISF with fast enough kinetics for adequate measurement time-lag?
Biofluid	Considering current knowledge of the benefits and challenges of measuring analytes in ISF, is there a compelling benefit (such as lower invasiveness, continuous measuring or greater accuracy) to sensing ISF rather than other biofluids?
Sensor or assay	Can the sensor measure endogenous or dosed levels of the target analyte and their changes? Considering the relevant potential confounding factors (such as interfering solutes, temperature or motion), can the sensor specifically and selectively measure the analyte of choice in vivo? Does the sensor lag-time meet temporal requirements for continuous monitoring or for time-to-answer? For continuous monitoring, can the sensor function robustly in vivo over a timespan that maximizes benefits and minimizes costs? If an extraction-based assay is used, and given the typically small volumes of ISF extracted, does the assay satisfy the required sensitivity, specificity, selectivity and limit of detection?

In fact, the opportunities are plenty: ongoing advancements are yielding biosensors with improved performance and functionality[99], and technology that can sensitively and continuously monitor biomarkers in ISF may one day revolutionize molecular diagnostics and the monitoring of physiological states with molecular precision.

References

1. Tobias, A., Ballard, B. D. & Mohiuddin, S. S. *Physiology, Water Balance* (StatPearls Publishing LLC, updated 3 October 2022); https://www.ncbi.nlm.nih.gov/books/NBK541059/
2. Ash, S. R. et al. Subcutaneous capillary filtrate collector for measurement of blood glucose. *ASAIO J.* **38**, M416–M420 (1992).
3. Gebhart, S. et al. Glucose sensing in transdermal body fluid collected under continuous vacuum pressure via micropores in the stratum corneum. *Diabetes Technol. Ther.* **5**, 159–166 (2003).
4. Miller, P. R. et al. Extraction and biomolecular analysis of dermal interstitial fluid collected with hollow microneedles. *Commun. Biol.* **1**, 173 (2018).
5. Tran, B. Q. et al. Proteomic characterization of dermal interstitial fluid extracted using a novel microneedle-assisted technique. *J. Proteome Res.* **17**, 479–485 (2018).
6. Taylor, R. M., Miller, P. R., Ebrahimi, P., Polsky, R. & Baca, J. T. Minimally-invasive, microneedle-array extraction of interstitial fluid for comprehensive biomedical applications: transcriptomics, proteomics, metabolomics, exosome research, and biomarker identification. *Lab. Anim.* **52**, 526–530 (2018).
7. Aukland, K. & Reed, R. K. Interstitial-lymphatic mechanisms in the control of extracellular fluid volume. *Physiol. Rev.* **73**, 1–78 (1993).
8. Vermeer, B. J., Reman, F. C. & van Gent, C. M. The determination of lipids and proteins in suction blister fluid. *J. Invest. Dermatol.* **73**, 303–305 (1979).
9. Rodbard, D. Continuous glucose monitoring: a review of successes, challenges, and opportunities. *Diabetes Technol. Ther.* **18** (Suppl. 2), S3–S13 (2016).
10. Heikenfeld, J. et al. Accessing analytes in biofluids for peripheral biochemical monitoring. *Nat. Biotechnol.* **37**, 407–419 (2019).
11. Reed, R. K. & Rubin, K. Transcapillary exchange: role and importance of the interstitial fluid pressure and the extracellular matrix. *Cardiovasc. Res.* **87**, 211–217 (2010).
12. Madden, J., O'Mahony, C., Thompson, M., O'Riordan, A. & Galvin, P. Biosensing in dermal interstitial fluid using microneedle based electrochemical devices. *Sens. Biosens. Res.* **29**, 100348 (2020).
13. Kashaninejad, N. et al. Microneedle arrays for sampling and sensing skin interstitial fluid. *Chemosensors* **9**, 83 (2021).
14. García-Guzmán, J. J., Pérez-Ràfols, C., Cuartero, M. & Crespo, G. A. Microneedle based electrochemical (bio)sensing: towards decentralized and continuous health status monitoring. *Trends Anal. Chem.* **135**, 116148 (2021).
15. Kiang, T. K. L., Ranamukhaarachchi, S. A. & Ensom, M. H. H. Revolutionizing therapeutic drug monitoring with the use of interstitial fluid and microneedles technology. *Pharmaceutics* **9**, 43 (2017).
16. Kretsos, K. & Kasting, G. B. Dermal capillary clearance: physiology and modeling. *Skin Pharmacol. Physiol.* **18**, 55–74 (2005).
17. Groenendaal, W., von Basum, G., Schmidt, K. A., Hilbers, P. A. J. & van Riel, N. A. W. Quantifying the composition of human skin for glucose sensor development. *J. Diabetes Sci. Technol.* **4**, 1032–1040 (2010).
18. Liao, Y.-H. et al. Quantitative analysis of intrinsic skin aging in dermal papillae by in vivo harmonic generation microscopy. *Biomed. Opt. Express* **5**, 3266–3279 (2014).
19. Levick, J. R. Flow through interstitium and other fibrous matrices. *Q. J. Exp. Physiol.* **72**, 409–437 (1987).
20. Wiig, H. & Swartz, M. A. Interstitial fluid and lymph formation and transport: physiological regulation and roles in inflammation and cancer. *Physiol. Rev.* **92**, 1005–1060 (2012).
21. Skobe, M. & Detmar, M. Structure, function, and molecular control of the skin lymphatic system. *J. Investig. Dermatol. Symp. Proc.* **5**, 14–19 (2000).
22. Shore, A. C. Capillaroscopy and the measurement of capillary pressure. *Br. J. Clin. Pharm.* **50**, 501–513 (2000).
23. Stewart, R. H. A modern view of the interstitial space in health and disease. *Front. Vet. Sci.* **7**, 609583 (2020).
24. Jamalian, S. et al. Demonstration and analysis of the suction effect for pumping lymph from tissue beds at subatmospheric pressure. *Sci. Rep.* **7**, 12080 (2017).
25. Levick, J. R. & Michel, C. C. Microvascular fluid exchange and the revised Starling principle. *Cardiovasc. Res.* **87**, 198–210 (2010).
26. Ibrahim, R., Nitsche, J. M. & Kasting, G. B. Dermal clearance model for epidermal bioavailability calculations. *J. Pharm. Sci.* **101**, 2094–2108 (2012).
27. Ono, S., Egawa, G. & Kabashima, K. Regulation of blood vascular permeability in the skin. *Inflamm. Regen.* **37**, 11 (2017).
28. Pries, A. R., Secomb, T. W. & Gaehtgens, P. The endothelial surface layer. *Pflügers Arch. Eur. J. Physiol.* **440**, 653–666 (2000).
29. Stan, R.-V. Structure and function of endothelial caveolae. *Microsc. Res. Tech.* **57**, 350–364 (2002).
30. Davis, M. J., Rahbar, E., Gashev, A. A., Zawieja, D. C. & Moore, J. E. Determinants of valve gating in collecting lymphatic vessels from rat mesentery. *Am. J. Physiol. Heart Circ. Physiol.* **301**, H48–H60 (2011).
31. Mendoza, E. & Schmid-Schönbein, G. W. A model for mechanics of primary lymphatic valves. *J. Biomech. Eng.* **125**, 407–414 (2003).

32. Suami, H. & Scaglioni, M. F. Anatomy of the lymphatic system and the lymphosome concept with reference to lymphedema. *Semin. Plast. Surg.* **32**, 5–11 (2018).
33. Bendayan, M. Morphological and cytochemical aspects of capillary permeability. *Microsc. Res. Tech.* **57**, 327–349 (2002).
34. Shen, L., Weber, C. R. & Turner, J. R. The tight junction protein complex undergoes rapid and continuous molecular remodeling at steady state. *J. Cell Biol.* **181**, 683–695 (2008).
35. Anderson, J. M. & Van Itallie, C. M. Physiology and function of the tight junction. *Cold Spring Harb. Perspect. Biol.* **1**, a002584 (2009).
36. Rippe, B. & Haraldsson, B. Transport of macromolecules across microvascular walls: the two-pore theory. *Physiol. Rev.* **74**, 163–219 (1994).
37. Rutili, G. & Arfors, K. E. Protein concentration in interstitial and lymphatic fluids from the subcutaneous tissue. *Acta Physiol. Scand.* **99**, 1–8 (1977).
38. Haaverstad, R., Romslo, I., Larsen, S. & Myhre, H. O. Protein concentration of subcutaneous interstitial fluid in the human leg. *Int. J. Microcirc. Clin. Exp.* **16**, 111–117 (1996).
39. Michel, C. C. & Curry, F. E. Microvascular permeability. *Physiol. Rev.* **79**, 703–761 (1999).
40. Vink, H. & Duling, B. R. Capillary endothelial surface layer selectively reduces plasma solute distribution volume. *Am. J. Physiol. Heart Circ. Physiol.* **278**, H285–H289 (2000).
41. Yuan, Y. et al. Oil-membrane protection of electrochemical sensors for fouling- and pH-insensitive detection of lipophilic analytes. *ACS Appl. Mater. Interfaces* **13**, 53553–53563 (2021).
42. Norvaisas, P. & Ziemys, A. The role of payload hydrophobicity in nanotherapeutic pharmacokinetics. *J. Pharm. Sci.* **103**, 2147–2156 (2014).
43. Veber, D. F. et al. Molecular properties that influence the oral bioavailability of drug candidates. *J. Med. Chem.* **45**, 2615–2623 (2002).
44. Bhake, R. et al. Continuous free cortisol profiles in healthy men: validation of microdialysis method. *J. Clin. Endocrinol. Metab.* **105**, e1749–e1761 (2020).
45. Zhang, F., Xue, J., Shao, J. & Jia, L. Compilation of 222 drugs' plasma protein binding data and guidance for study designs. *Drug Discov. Today* **17**, 475–485 (2012).
46. Liebl, H. & Kloth, L. C. Skin cell proliferation stimulated by microneedles. *J. Am. Coll. Clin. Wound Spec.* **4**, 2–6 (2012).
47. Egawa, G. et al. Intravital analysis of vascular permeability in mice using two-photon microscopy. *Sci. Rep.* **3**, 1932 (2013).
48. Ripolin, A. et al. Successful application of large microneedle patches by human volunteers. *Int. J. Pharm.* **521**, 92–101 (2017).
49. Nickoloff, B. J. & Naidu, Y. Perturbation of epidermal barrier function correlates with initiation of cytokine cascade in human skin. *J. Am. Acad. Dermatol.* **30**, 535–546 (1994).
50. Clough, G. F., Jackson, C. L., Lee, J. J. P., Jamal, S. C. & Church, M. K. What can microdialysis tell us about the temporal and spatial generation of cytokines in allergen-induced responses in human skin in vivo? *J. Invest. Dermatol.* **127**, 2799–2806 (2007).
51. Kolluru, C. et al. Monitoring drug pharmacokinetics and immunologic biomarkers in dermal interstitial fluid using a microneedle patch. *Biomed. Microdevices* **21**, 14 (2019).
52. Blicharz, T. M. et al. Microneedle-based device for the one-step painless collection of capillary blood samples. *Nat. Biomed. Eng.* **2**, 151–157 (2018).
53. Svedman, C., Yu, B. B., Ryan, T. J. & Svensson, H. Plasma proteins in a standardised skin mini-erosion (I): permeability changes as a function of time. *BMC Dermatol.* **2**, 3 (2002).
54. Svedman, C., Yu, B. B., Ryan, T. J. & Svensson, H. Plasma proteins in a standardised skin mini-erosion (II): effects of extraction pressure. *BMC Dermatol.* **2**, 4 (2002).
55. Stout, P. et al. Site-to-site variation of glucose in interstitial fluid samples and correlation to venous plasma glucose. *Clin. Chem.* **45**, 1674–1675 (1999).
56. Kramer, G. C., Sibley, L., Aukland, K. & Renkin, E. M. Wick sampling of interstitial fluid in rat skin: further analysis and modifications of the method. *Microvasc. Res.* **32**, 39–49 (1986).
57. Noddeland, H. Colloid osmotic pressure of human subcutaneous interstitial fluid sampled by nylon wicks: evaluation of the method. *Scand. J. Clin. Lab. Invest.* **42**, 123–130 (1982).
58. Wiig, H., Heir, S. & Aukland, K. Colloid osmotic pressure of interstitial fluid in rat subcutis and skeletal muscle: comparison of various wick sampling techniques. *Acta Physiol. Scand.* **133**, 167–175 (1988).
59. Samant, P. P. & Prausnitz, M. R. Mechanisms of sampling interstitial fluid from skin using a microneedle patch. *Proc. Natl Acad. Sci. USA* **115**, 4583–4588 (2018).
60. Laszlo, E., De Crescenzo, G., Nieto-Argüello, A., Banquy, X. & Brambilla, D. Superswelling microneedle arrays for dermal interstitial fluid (prote)omics. *Adv. Funct. Mater.* **31**, 2106061 (2021).
61. Woodley, D. et al. Localization of basement membrane components after dermal-epidermal junction separation. *J. Invest. Dermatol.* **81**, 149–153 (1983).
62. Samant, P. P. et al. Sampling interstitial fluid from human skin using a microneedle patch. *Sci. Transl Med.* **12**, eaaw0285 (2020).
63. Korf, J., Huinink, K. D. & Posthuma-Trumpie, G. A. Ultraslow microdialysis and microfiltration for in-line, on-line and off-line monitoring. *Trends Biotechnol.* **28**, 150–158 (2010).
64. Chaurasia, C. S. et al. AAPS-FDA workshop white paper: microdialysis principles, application and regulatory perspectives. *Pharm. Res.* **24**, 1014–1025 (2007).
65. Nightingale, A. M. et al. Monitoring biomolecule concentrations in tissue using a wearable droplet microfluidic-based sensor. *Nat. Commun.* **10**, 2741 (2019).
66. Collison, M. E. et al. Analytical characterization of electrochemical biosensor test strips for measurement of glucose in low-volume interstitial fluid samples. *Clin. Chem.* **45**, 1665–1673 (1999).
67. Wang, Z. et al. Microneedle patch for the ultrasensitive quantification of protein biomarkers in interstitial fluid. *Nat. Biomed. Eng.* **5**, 64–76 (2021).
68. Zheng, H. et al. Hydrogel microneedle-assisted assay integrating aptamer probes and fluorescence detection for reagentless biomarker quantification. *ACS Sens.* **7**, 2387–2399 (2022).
69. Bouissou, C. C., Sylvestre, J.-P., Guy, R. H. & Delgado-Charro, M. B. Reverse iontophoresis of amino acids: identification and separation of stratum corneum and subdermal sources in vitro. *Pharm. Res.* **26**, 2630–2638 (2009).
70. Tierney, M. J. et al. Design of a biosensor for continual, transdermal glucose monitoring. *Clin. Chem.* **45**, 1681–1683 (1999).
71. Cengiz, E. & Tamborlane, W. V. A tale of two compartments: interstitial versus blood glucose monitoring. *Diabetes Technol. Ther.* **11**, S11–S16 (2009).
72. Chen, C. et al. Recent advances in electrochemical glucose biosensors: a review. *RSC Adv.* **3**, 4473–4491 (2013).
73. Hirsch, I. B. & Wright, E. E. Using flash continuous glucose monitoring in primary practice. *Clin. Diabetes* **37**, 150–161 (2019).
74. McClatchey, P. M. et al. Fibrotic encapsulation is the dominant source of continuous glucose monitor delays. *Diabetes* **68**, 1892–1901 (2019).
75. Hoath, S. B. & Leahy, D. G. The organization of human epidermis: functional epidermal units and phi proportionality. *J. Invest. Dermatol.* **121**, 1440–1446 (2003).

76. Garg, S. K. et al. Evaluation of accuracy and safety of the next-generation up to 180-day long-term implantable eversense continuous glucose monitoring system: the PROMISE study. *Diabetes Technol. Ther.* https://doi.org/10.1089/dia.2021.0182 (2021).
77. Boscari, F. et al. Implantable and transcutaneous continuous glucose monitoring system: a randomized cross over trial comparing accuracy, efficacy and acceptance. *J. Endocrinol. Invest*. https://doi.org/10.1007/s40618-021-01624-2 (2021).
78. Christiansen, M. P. et al. A prospective multicenter evaluation of the accuracy and safety of an implanted continuous glucose sensor: the PRECISION study. *Diabetes Technol. Ther.* **21**, 231–237 (2019).
79. Wan, W. et al. Cost-effectiveness of continuous glucose monitoring for adults with type 1 diabetes compared with self-monitoring of blood glucose: the DIAMOND randomized trial. *Diabetes Care* **41**, 1227–1234 (2018).
80. Hoskins, M. & Tenderich, A. Senseonics stops sales of eversense implantable CGM in wake of COVID-19 crisis. *Healthline* (31 March 2020); https://www.healthline.com/diabetesmine/senseonics-suspends-eversense-implantable-cgm
81. Joseph, J. I. Review of the long-term implantable senseonics continuous glucose monitoring system and other continuous glucose monitoring systems. *J. Diabetes Sci. Technol.* **15**, 167–173 (2021).
82. Kanick, S. C., Schneider, P. A., Klitzman, B., Wisniewski, N. A. & Rebrin, K. Continuous monitoring of interstitial tissue oxygen using subcutaneous oxygen microsensors: in vivo characterization in healthy volunteers. *Microvasc. Res.* **124**, 6–18 (2019).
83. Gill, H. S., Denson, D. D., Burris, B. A. & Prausnitz, M. R. Effect of microneedle design on pain in human subjects. *Clin. J. Pain* **24**, 585–594 (2008).
84. Levin, Y., Kochba, E., Hung, I. & Kenney, R. Intradermal vaccination using the novel microneedle device MicronJet600: past, present, and future. *Hum. Vaccin. Immunother.* **11**, 991–997 (2015).
85. Leone, M. et al. Universal applicator for digitally-controlled pressing force and impact velocity insertion of microneedles into skin. *Pharmaceutics* **10**, 211 (2018).
86. Rawson, T. M. et al. Microneedle biosensors for real-time, minimally invasive drug monitoring of phenoxymethylpenicillin: a first-in-human evaluation in healthy volunteers. *Lancet Digit. Health* **1**, e335–e343 (2019).
87. Jina, A. et al. Design, development, and evaluation of a novel microneedle array-based continuous glucose monitor. *J. Diabetes Sci. Technol.* **8**, 483–487 (2014).
88. Tehrani, F. et al. An integrated wearable microneedle array for the continuous monitoring of multiple biomarkers in interstitial fluid. *Nat. Biomed. Eng*. https://doi.org/10.1038/s41551-022-00887-1 (2022).
89. Wu, Y. et al. Microneedle aptamer-based sensors for continuous, real-time therapeutic drug monitoring. *Anal. Chem*. https://doi.org/10.1021/acs.analchem.2c00829 (2022).
90. Lin, S. et al. Wearable microneedle-based electrochemical aptamer biosensing for precision dosing of drugs with narrow therapeutic windows. *Sci. Adv.* **8**, eabq4539 (2022).
91. Spehar-Délèze, A.-M., Anastasova, S. & Vadgama, P. Monitoring of lactate in interstitial fluid, saliva and sweat by electrochemical biosensor: the uncertainties of biological interpretation. *Chemosensors* **9**, 195 (2021).
92. Kretsos, K., Miller, M. A., Zamora-Estrada, G. & Kasting, G. B. Partitioning, diffusivity and clearance of skin permeants in mammalian dermis. *Int. J. Pharm.* **346**, 64–79 (2008).
93. Heikenfeld, J. et al. Wearable sensors: modalities, challenges, and prospects. *Lab Chip* **18**, 217–248 (2018).
94. Rocchitta, G. et al. Enzyme biosensors for biomedical applications: strategies for safeguarding analytical performances in biological fluids. *Sensors* **16**, 780 (2016).
95. Maahs, D. M. et al. Effect of acetaminophen on CGM glucose in an outpatient setting. *Diabetes Care* **38**, e158–e159 (2015).
96. Arroyo-Currás, N., Dauphin-Ducharme, P., Scida, K. & Chávez, J. L. From the beaker to the body: translational challenges for electrochemical, aptamer-based sensors. *Anal. Methods* **12**, 1288–1310 (2020).
97. Leung, K. K., Downs, A. M., Ortega, G., Kurnik, M. & Plaxco, K. W. Elucidating the mechanisms underlying the signal drift of electrochemical aptamer-based sensors in whole blood. *ACS Sens.* **6**, 3340–3347 (2021).
98. Shaver, A. & Arroyo-Currás, N. The challenge of long-term stability for nucleic acid-based electrochemical sensors. *Curr. Opin. Electrochem.* **32**, 100902 (2022).
99. Watkins, Z., Karajić, A., Young, T., White, R. & Heikenfeld, J. Week-long operation of electrochemical aptamer sensors: new insights into self-assembled monolayer degradation mechanisms and solutions for stability in biofluid at body temperature. Preprint at *ChemRxiv* https://doi.org/10.26434/chemrxiv-2022-s1qj9 (2022).
100. Kurnik, M., Pang, E. Z. & Plaxco, K. W. An electrochemical biosensor architecture based on protein folding supports direct real-time measurements in whole blood. *Angew. Chem. Int. Ed.* **59**, 18442–18445 (2020).
101. Dauphin-Ducharme, P. et al. Electrochemical aptamer-based sensors for improved therapeutic drug monitoring and high-precision, feedback-controlled drug delivery. *ACS Sens.* **4**, 2832–2837 (2019).
102. Chien, J.-C., Baker, S. W., Soh, H. T. & Arbabian, A. Design and analysis of a sample-and-hold CMOS electrochemical sensor for aptamer-based therapeutic drug monitoring. *IEEE J. Solid State Circuits* **55**, 2914–2929 (2020).
103. Mage, P. L. et al. Closed-loop control of circulating drug levels in live animals. *Nat. Biomed. Eng.* **1**, 0070 (2017).
104. Ye, Z.-K., Tang, H.-L. & Zhai, S.-D. Benefits of therapeutic drug monitoring of vancomycin: a systematic review and meta-analysis. *PLoS ONE* **8**, e77169 (2013).
105. Roberts, J. A., Norris, R., Paterson, D. L. & Martin, J. H. Therapeutic drug monitoring of antimicrobials. *Br. J. Clin. Pharmacol.* **73**, 27–36 (2012).
106. Sime, F. B., Roberts, M. S., Peake, S. L., Lipman, J. & Roberts, J. A. Does beta-lactam pharmacokinetic variability in critically ill patients justify therapeutic drug monitoring? A systematic review. *Ann. Intensive Care* **2**, 35 (2012).
107. Ates, H. C. et al. On-site therapeutic drug monitoring. *Trends Biotechnol.* **38**, 1262–1277 (2020).
108. Kiang, T. K. L., Häfeli, U. O. & Ensom, M. H. H. A comprehensive review on the pharmacokinetics of antibiotics in interstitial fluid spaces in humans: implications on dosing and clinical pharmacokinetic monitoring. *Clin. Pharmacokinet.* **53**, 695–730 (2014).
109. Harbarth, S., Samore, M. H., Lichtenberg, D. & Carmeli, Y. Prolonged antibiotic prophylaxis after cardiovascular surgery and its effect on surgical site infections and antimicrobial resistance. *Circulation* **101**, 2916–2921 (2000).
110. Skhirtladze, K. et al. Impaired target site penetration of vancomycin in diabetic patients following cardiac surgery. *Antimicrob. Agents Chemother.* **50**, 1372–1375 (2006).
111. Hamada, Y., Kuti, J. L. & Nicolau, D. P. Vancomycin serum concentrations do not adequately predict tissue exposure in diabetic patients with mild to moderate limb infections. *J. Antimicrob. Chemother.* **70**, 2064–2067 (2015).

112. Paneni, F., Beckman, J. A., Creager, M. A. & Cosentino, F. Diabetes and vascular disease: pathophysiology, clinical consequences, and medical therapy: part I. *Eur. Heart J.* **34**, 2436–2443 (2013).
113. Kennedy, J. M. & Van Riji, A. M. Effects of surgery on the pharmacokinetic parameters of drugs. *Clin. Pharmacokinet.* **35**, 293–312 (1998).
114. De Paepe, P., Belpaire, F. M. & Buylaert, W. A. Pharmacokinetic and pharmacodynamic considerations when treating patients with sepsis and septic shock. *Clin. Pharmacokinet.* **41**, 1135–1151 (2002).
115. Blot, S. I., Pea, F. & Lipman, J. The effect of pathophysiology on pharmacokinetics in the critically ill patient — concepts appraised by the example of antimicrobial agents. *Adv. Drug Deliv. Rev.* **77**, 3–11 (2014).
116. LaCount, T. D. et al. Modeling temperature-dependent dermal absorption and clearance for transdermal and topical drug applications. *AAPS J.* **22**, 70 (2020).
117. Riviere, J. E. & Williams, P. L. Pharmacokinetic implications of changing blood flow in skin. *J. Pharm. Sci.* **81**, 601–602 (1992).
118. Barre, J., Didey, F., Delion, F. & Tillement, J.-P. Problems in therapeutic drug monitoring: free drug level monitoring. *Ther. Drug Monit.* **10**, 133–143 (1988).
119. Zeitlinger, M. A. et al. Protein binding: do we ever learn? *Antimicrob. Agents Chemother.* **55**, 3067–3074 (2011).
120. Butterfield, J. M. et al. Refining vancomycin protein binding estimates: identification of clinical factors that influence protein binding. *Antimicrob. Agents Chemother.* **55**, 4277–4282 (2011).
121. Tisoncik, J. R. et al. Into the eye of the cytokine storm. *Microbiol. Mol. Biol. Rev.* **76**, 16–32 (2012).
122. Guo, Y.-R. et al. The origin, transmission and clinical therapies on coronavirus disease 2019 (COVID-19) outbreak – an update on the status. *Mil. Med. Res.* **7**, 11 (2020).
123. Schulert, G. S. & Grom, A. A. Pathogenesis of macrophage activation syndrome and potential for cytokine-directed therapies. *Annu. Rev. Med.* **66**, 145–159 (2015).
124. Nestle, F. O., Di Meglio, P., Qin, J.-Z. & Nickoloff, B. J. Skin immune sentinels in health and disease. *Nat. Rev. Immunol.* **9**, 679–691 (2009).
125. Clark, R. A. et al. The vast majority of CLA+ T cells are resident in normal skin. *J. Immunol.* **176**, 4431–4439 (2006).
126. Nedrebø, T., Reed, R. K., Jonsson, R., Berg, A. & Wiig, H. Differential cytokine response in interstitial fluid in skin and serum during experimental inflammation in rats. *J. Physiol.* **556**, 193–202 (2004).
127. Zaleska, M., Olszewski, W. L., Durlik, M. & Miller, N. E. Signaling proteins are represented in tissue fluid/lymph from soft tissues of normal human legs at concentrations different from serum. *Lymphat. Res. Biol.* **11**, 203–210 (2013).
128. Kumar, A. et al. Duration of hypotension before initiation of effective antimicrobial therapy is the critical determinant of survival in human septic shock. *Crit. Care Med.* **34**, 1589–1596 (2006).
129. Panelli, M. C. et al. Forecasting the cytokine storm following systemic interleukin (IL)-2 administration. *J. Transl Med.* **2**, 17 (2004).

Acknowledgements

The authors at the University of Cincinnati acknowledge support from the US Air Force Office of Scientific Research (USAF Contract No. FA9550-20-1-0117), a National Science Foundation CBET Award (No. 2125056), a National Science Foundation ECCS Award (No. 2025720) and a US Office of Naval Research Award (No. N00014-20-1-2764). The authors at Stanford University thank M. Eisenstein for his editorial contributions, and appreciate financial support from W. L Gore and Associates, the Helmsley Trust and the National Institutes of Health (NIH, OT2OD025342). I.A.P.T. acknowledges support from the Medtronic Foundation Stanford Graduate Fellowship and from the Natural Sciences and Engineering Research Council of Canada (NSERC, 416353855). Sandia National Laboratories is a multimission laboratory managed and operated by National Technology and Engineering Solutions of Sandia, LLC, a wholly owned subsidiary of Honeywell International Inc., for the US Department of Energy's National Nuclear Security Administration under contract DE-NA0003525. This Perspective describes objective technical results and analysis. Any subjective views or opinions that might be expressed here do not necessarily represent the views of the US Department of Energy or the United States Government.

Author contributions

M.F. and I.A.P.T. contributed equally to writing and revising all sections. G.K. contributed to the writing of the sections 'Structure and composition of the dermis' and 'Partitioning of analytes in dermal ISF'. R.P. contributed to the sections 'Partitioning of analytes in dermal ISF' and 'Applications of ISF in diagnostics'. D.C. contributed to the section 'Challenges in obtaining true ISF via extraction'. J.H. and H.T.S led the project and contributed to the writing and revision of all sections.

Competing interests

J.H. is a co-founder of Kilele Health Inc., which is pursuing the commercialization of wearables for the continuous monitoring of analytes in ISF. H.T.S. is a co-founder of Eigen Biosciences, which seeks to commercialize technologies for measuring biomarkers in ISF. The other authors declare no competing interests.

Additional information

Supplementary information The online version contains supplementary material available at https://doi.org/10.1038/s41551-022-00998-9.

Correspondence should be addressed to Hyongsok Tom Soh or Jason Heikenfeld.

Peer review information *Nature Biomedical Engineering* thanks Srikanth Singamaneni and the other, anonymous, reviewer(s) for their contribution to the peer review of this work.